proceedings

MDPI

Proceedings

Building Up Co-Crystals: Structural Motif Consistencies Across Families of Co-Crystals †

Colin C. Seaton

School of Chemistry and Biosciences, University of Bradford, Richmond Road, Bradford BD7 1DP, UK; c.seaton@bradford.ac.uk; Tel.: +44-1274-236165

† Presented at the 1st International Electronic Conference on Pharmaceutics, 1–15 December 2020; Available online: https://iecp2020.sciforum.net/.

Received: date; Accepted: date; Published: date

Abstract: The creation of co-crystals as a route to create new pharmaceutical phases with modified or defined physicochemical properties is an area of intense research. Much of the current research has focused on creating new phases for numerous active pharmaceutical ingredients (APIs) to alter physical properties such as low solubilities, enhancing processability or stability. Such studies have identified suitable co-formers and common bonding motifs to aid with the design of new co-crystals but understanding how the changes in molecular structure of the components are reflected in the packing and resulting properties is still lacking. This lack of insight means that the design and growth of new co-crystals is still a largely empirical process with co-formers selected and then attempts to grow the different materials undertaken to evaluate the resulting properties. This work will report on the results of a combination of crystal structure database analysis with computational chemistry studies to identify what structural features are retained across a selection of families of co-crystals with common components. The competition between different potential hydrogen bonding motifs was evaluated using ab initio quantum mechanical calculations and this was related to the commonality in the packing motifs when observed. It is found while the stronger local bonding motifs are often retained within systems, the balance of weaker long-range packing forces gives rise to many subtle shifts in packing leading to greater challenges in the prediction of final crystal structures.

Keywords: co-crystals; crystal engineering; crystal structure prediction; hydrogen bonding; intermolecular interactions

1. Introduction

Modifying the physicochemical properties of active pharmaceutical ingredients (APIs) through the creation of multi-component crystals (i.e., co-crystals and salts) is a rapidly developing field of study [1]. They have been primarily investigated to adjust solubility and so increase bioavailability[2], but other studies have also included increased stability under storage conditions, improved tableting performance or processability [3,4]. Such studies are often empirically driven with screening of standard co-formers under a range of experimental conditions used to locate new potential phases before undertaking evaluation of the physical properties [5]. Co-formers are frequently chosen by consideration of potential supramolecular synthons that could form between the components [6]. Many potential co-formers offer a number of potential supramolecular synthons and it is not always predictable which will from and how these will lead to desirable properties. One route to achieve this understanding is to undertake data mining exercises into the existing crystal structures from families of multi-component crystals with common structural features throughout the set and identify if there are relationships in the component choice and the resulting crystal structures [7–9].

Computational chemistry approaches offer key information to aid with these studies as the intermolecular interactions within known crystal structures, predicted crystal structures or

supramolecular motifs can be readily evaluated. Studies into the formation thermodynamics of co-crystal and salts are limited, however the majority of multi-component crystals are dominated by the enthalpic component [10,11]. Analysis of lattice energy components indicates two or three close contacts dominate the energy. This suggests that an initial screening could be based on the interactions between the components [12]. For this to be effective suitable bonding motifs need to be identified or predicted for a given system.

Isonicotinamide (INA) and nicotinamide (NA) are frequently used co-formers, both for modification of API's physicochemical properties [13,14] and as model systems for co-crystallization studies [15,16]. Both INA and NA offer one hydrogen bond donor/acceptor group ($CONH_2$) and one hydrogen bond acceptor (N_{pyr}) but in different orientations, this allows for studies into the influence on relative positioning on the final crystal packing. Thus, there are only three potential interactions with suitable hydrogen bond donor groups such as CO_2H or OH groups (**Error! Reference source not found.**). Previous studies indicate a preference for the binding between co-formers and the pyridine nitrogen in most co-crystals [17], however it would be expected for carboxylic acids that the acid… amide motif should be lowered in energy as it comprises two hydrogen bonds. It has been shown for the acid amide interaction in benzoic acid-benzamide co-crystals that the strength of this interaction depends on the nature of the functional groups present [18] and so the changes in the balance between these interactions will be investigated to identify the interplay between the nature of the other functional groups present in the molecule.

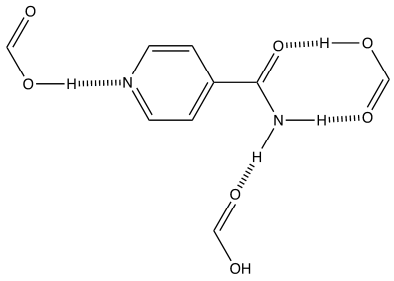

Figure 1. Three hydrogen bonding sites in INA with carboxylic acid group.

2. Computational Methodology

The crystal structures of isonicotinamide and nicotinamide were located in the Cambridge Structural Database (V5.41) [19] using Conquest (V2020.2.0) [20]. The crystal structure analysis (identification of hydrogen bonding, graph set determination, crystal structure similarity matching) was carried out using Mercury (V2020.2.0) [21–23].

Intermolecular hydrogen bonding motifs were identified in the various structures, extracted from the crystal structures and optimized at the DFT level (TPSS-D/def2-TZVP) [24–27] using the program orca. The interaction energy for these systems were then evaluated in orca [28] at the DFT (RI-PWPB95-D/ma-def2-QZVPP) [25,29]. The basis set superposition error was evaluated to be ~0.1 kJ mol^{-1} and so not included in calculations for tetramers and higher. Energy frameworks for selected crystal structure were evaluated in CrystalExplorer [30] using B3LYP/6-31G(d,p) DFT theory. Pairwise optimization of molecular components was carried out using the drift bias free differential evolution global optimization algorithm (Control parameters: K, F, G_{max}, N_p = 0.5, 0.98, 5000, 120) [31] using the AA-CLP force field [32] to evaluate the interaction energy between the molecules.

3. Results and Discussion

3.1. Co-former and Compositional Analysis

A total of 215 isonicotinamide and 158 nicotinamide multi-component crystals were located and grouped based on the functional group hydrogen bonding to the pyridine nitrogen), the numbers of different compositions were also identified. The results show that the distribution is similar for either co-former. NA systems have a higher proportion of compositions compared to INA, which may be just to the relative bent geometry of NA functional compared to the linear location in INA. There may be a preference for (1:1) compositions, but this may reflect the screening approaches used and the higher composition systems may be harder to grow compared to the (1:1) composition. It has been reported that the (2:1) benzoic acid-INA co-crystal is metastable compared to the (1:1) and only forms under limited experimental conditions[15,33].

Table 1. Number of INA containing systems for a given linking motif in different compositions (Co-former:INA) ratio.

Class	(1:1)	(2:1)	(1:2)	(1:1:1)	Other Compositions §	Totals
$ArCO_2H\cdots INA$	44	9	5	15	1	74 (34%)
$RCO_2H\cdots INA$	44	3	22	2	0	71 (33%)
ROH···INA	18	1	10	1	4	34 (16%)
Other Functional Groups	22	2	4	6	2	36 (17%)
Totals	128 (60%)	15 (7%)	41 (19%)	24 (11%)	7 (3%)	**215**

§ Compositions are (1:1:1:1), (1:2:1.7), (1:3:2), (1:2:2), (3:2), (2:1:2).

Table 2. Number of NA containing systems for a given linking motif in different compositions (Co-former:INA) ratio.

Class	(1:1)	(2:1)	(1:2)	(1:1:1)	Other Compositions §	Totals
$ArCO_2H\cdots NA$	30	3	3	10	3	49 (31%)
$RCO_2H\cdots NA$	27	3	9	5	4	48 (30%)
ROH···NA	17	2	6	2	6	33 (21%)
Other Functional Groups	16	1	3	4	4	28 (18%)
Totals	90 (58%)	9 (6%)	21 (13%)	21 (13%)	17 (10%)	**158**

§ Compositions are (1:3), (1:4), (1:1:2), (1:1:5), (1:2:1), (1:4:1), (2:2:1), (2:2:1.25), (2:4:1), (4:4:3), (2:1:1:4).

The competition between functional groups was evaluated by considering the types of potential hydrogen bond donor groups present in the co-formers and the relative compositions formed (**Error! Reference source not found.**). Single functional group types form the majority of systems and dominate the (1:1) composition systems as expected. The (1:2) composition systems are dominated by molecules with multiple functional groups as 37/41 INA systems and 14/20 NA systems are classified as such. In contrast the (2:1) systems generally have a single functional group present and both groups bind to different sites on the INA/NA molecules.

Table 3. Numbers of Hydrogen Bond Donating Functional Groups Present in Different Compositions of INA/NA Co-Crystals. First group in pair bonds to the pyridine N.

Groups—INA	(1:1)	(2:1)	(1:2)	Groups—NA	(1:1)	(2:1)	(1:2)
CO_2H	69	6	22	CO_2H	36	4	11
CO_2H/OH	13	4	4	CO_2H/OH	14	2	1
CO_2H/NH_2	6	1	0	CO_2H/NH_2	3	0	0
CO_2H/CONHR	1	1	0	CO_2H/CONHR	1	0	0
CO_2H/SO_2NH_2	0	1	0	CO_2H/SO_2NH_2	2	0	1
OH	14	1	10	OH	15	1	4
OH/CO_2H	3	0	0	OH/CO_2H	2	0	0
OH/CONHR	2	0	0	OH/CONHR	0	0	1
$CONH_2$	4	1	0	$CONH_2$	2	1	2
SO_2NHR/CO_2H	1	0	1	SO_2NHR	3	0	0
NH_2	5	0	0	NH_2	3	0	0
All other functional groups	10	0	4	All other functional groups	8	0	1

3.2. Crystal Packing Analysis

(1:1) systems were selected for further analysis to identify repeating patterns in the bonding. Polymorphic systems were counted as separate systems as the hydrogen bonding motifs could be different in the different phases. First level graph set patterns were generated for each system (Table 1) to evaluate the differences between the phases.

Table 1. Frequencies of 1st level graph set motifs for INA and NA (1:1) co-crystals [§].

System	D(2)$R^2_2(8)$	D(2)$R^2_2(x)$	D(2)	D(2)C(x)
ArCO_2H---INA	41	0	2	1
RCO_2H---INA	20	0	21	3
ROH---INA	7	5	5	2
Other Functional Groups	9	0	4	10
Totals	**77 (59%)**	**5 (4%)**	**32 (25%)**	**16 (12%)**
ArCO_2H---NA	11	0	7	16
RCO_2H---NA	12	0	11	5
ROH---NA	5	0	8	7
Other Functional Groups	7	0	1	8
Totals	**35 (36%)**	**0 (0%)**	**27 (28%)**	**36 (36%)**

[§] x in graph set symbol indicates variable length of motif.

For INA, the dominant structure is a tetramer motif in 72% of the INA co-crystals (**Error! Reference source not found.**a). The remaining systems form a chain motif through two or more functional groups present in the co-former. In contrast, the opposite behaviour is observed in NA systems with only 36% of systems forming a tetramer motif (**Error! Reference source not found.**b). While the INA examples form planar structures, the motif in NA is twisted (the angle between benzoic acid and INA/NA molecular planes are 6° and 127° respectively). The carboxylic acid-INA systems show shifts in the form of this tetramer with 28% featuring a *cis* geometry between the carbonyl groups (**Error! Reference source not found.**). Polymorphic 2,4,6-trifluorobenzoic acid-isonicotinamide (PIRNOV) display both geometries in different phases. DFT energy calculations, show the *trans* geometry is lower by 2.15 kJ mol^{-1}. All bar one of the *cis* based tetramers form a consistent 3rd level hydrogen bonding motif forming a 1-D ladder structure built from a $R_6^6(26)$ motif (**Error! Reference source not found.**). The exception is form I of 5-chlorosalicylic acid (JIPJEQ) which forms a $C_2^2(11)$ motif instead. However, none of the 3-D structures display any further

packing similarities. Thus, the strongest interactions in the structure may be predictable, but the range of weaker packing forces can lead to a number of different crystal structures.

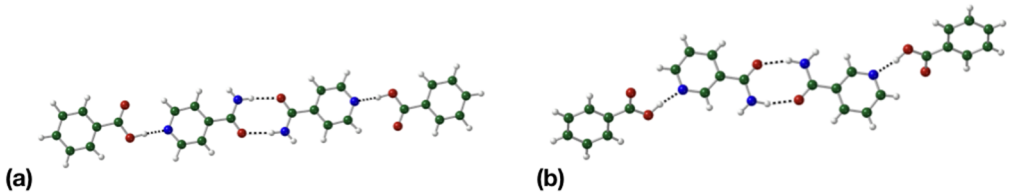

Figure 2. Formation of a tetramer in the (1:1) co-crystal between (**a**) benzoic acid-INA and (**b**) benzoic acid-NA.

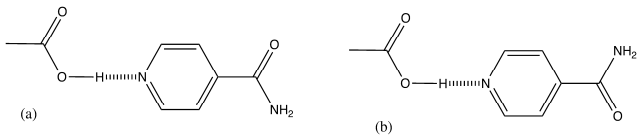

Figure 3. Chemical structures for the (**a**) *cis*- and (**b**) *trans*- geometry of acid-INA bonding.

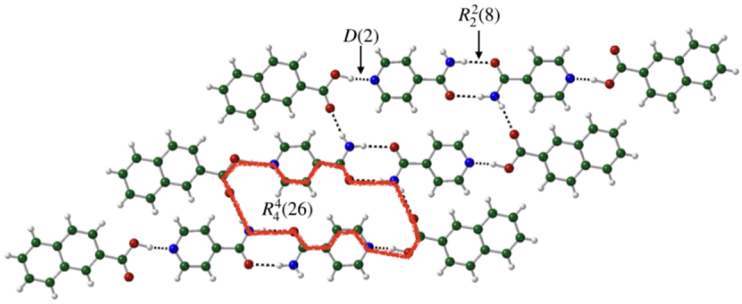

Figure 4. Formation of 1-D ladder structure in the 2-napthoic acid-INA co-crystal. The 3rd level hydrogen bond motif is highlighted in red.

The majority of *trans* systems can be classified into three sets: M2 has a 1-D ladder linked through a $R_4^4(22)$ motif (24/56 systems, Figure 1a), M3 an interlocked 3-D structure with $C_2^2(11)$ motifs (23/56 systems, Figure 1b), M4 links into a 1-D ladder through amide…amide ring with a $R_4^2(8)$ motif (4/56 systems, Figure 1c). The M2 set has three isostructural sets of structures, while 15 M3 structures pack in an isostructural set of C2/c structures, typified by benzoic acid (Figure 1b). The remaining groups have flatter angles. The M4 set splits into two isostructural subsets. This again confirms consistent local bonding but differences in longer packing is different.

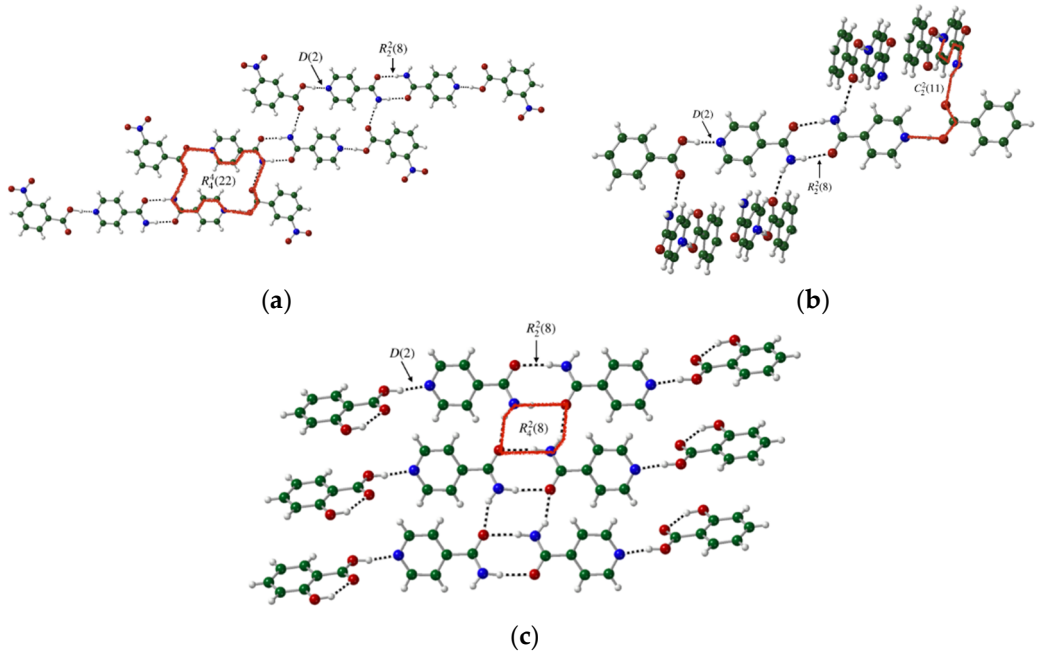

Figure 1. Example packings of tetramers form sets (**a**) M2, (**b**) M3 and (**c**) M4. Higher order hydrogen bonding motifs are highlighted in red.

3.3. Binding Interactions

The energy of intermolecular interactions within the (1:2) dicarboxylic acid-INA co-crystals were evaluated within CrystalExplorer. Summing the three strongest interactions in the structure (INA···INA, N-H···O=C, CO_2H···N_{pyr})) shows a general decrease with increasing chain length, however a slight odd-even alternation is noted (**Error! Reference source not found.**). Comparing this to the reported melting point shows a complementary pattern. However, the trend is not perfectly matched; there are two reported values for the melting point of the succinic acid co-crystal (135 °C [34] and 206 °C [35]) which affects the curves. Optimization of the position and orientation of molecules of oxalic acid with INA links the molecules through an acid···amide bond. This motif is not observed in any of the oxalic co-crystal structures but is lower in energy than the observed motif (

Table **2**). Evaluation of formation energy for the tetramer over two acid···amide dimers for a model system shows that the tetramer is favoured energetically by −26.74 kJ mol^{-1}. Thus, a set of slightly weaker interactions can give overall increased energy compared to the utilization of strongest possible interaction at each point. Similar evaluations for NA systems show similar energy values to INA ones and so the differences in packing appears to be dominated by the geometry and packing forces rather than preferential energetics.

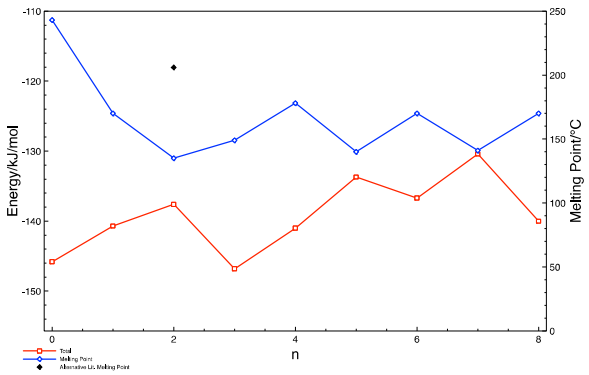

Figure 6. Plot of total interaction energies (red squares) and the reported melting points (blue circles) against chain length. Alterative literature melting point of succinic acid system is indicated by the black diamond.

Table 2. Energetics of acid…INA interactions at (RI-PWPB95-D/ma-def2-QZVPP) level of theory.

System	Acid…Amide Motif kJ mol^{-1}	Acid…Npyr Motif kJ mol^{-1}	Difference kJ mol^{-1}
Oxalic acid	−36.145	−32.556	−3.589
Malonic acid	−67.531	−51.742	−15.789
Succinic acid	−60.365	−45.143	−17.814
Glutaric acid	−61.957	−44.143	−16.959
Adipic acid	−57.152	−40.193	−16.959
Pimelic acid	−57.793	−50.027	−7.765
INA	−56.703	N/A	N/A

4. Conclusions

INA co-crystals and salts show consistent bonding features in the resulting crystal structures, with a common tetramer forming 72% of cases, in contrast NA only forms this motif in 36% of structures. Evaluation of the energy of the hydrogen bonds shows that in INA, while the stronger individual interactions can be predicted the combination of motifs in the tetramer gives a lower overall energy. This highlights that the balance between numerous factors dominates the co-crystallization processes. Comparing INA and NA system have similar energy values and so the differences in packing appear to be driven by the ability to pack efficiently in the crystal form rather than energetically. This indicates that to develop predictive methods based on pointwise contact location of the range of possibilities is more important compared to location of the global minimum interaction and evaluation of potential higher order building blocks will give insights into the resulting properties of the materials.

Conflicts of Interest: The authors declare no conflict of interest.

References

1. Bolla, G.; Nangia, A. Pharmaceutical cocrystals: Walking the talk. *Chem. Commun.* **2016**, *52*, 8342–8360.
2. Schultheiss, N.; Henck, J.-O. Role of Co-crystals in the Pharmaceutical Development Continuum. In *Pharmaceutical Salts and Co-Crystals*; Royal Society of Chemistry: Cambridge, UK, 2011; pp. 110–127.
3. Trask, A.V.; Motherwell, W.D.S.; Jones, W. Pharmaceutical Cocrystallization: Engineering a Remedy for Caffeine Hydration. *Cryst. Growth Des.* **2005**, *5*, 1013–1021.
4. Pagire, S.K.; Seaton, C.C.; Paradkar, A. Improving Stability of Effervescent Products by Co-Crystal Formation: A Novel Application of Crystal Engineered Citric Acid. *Cryst. Growth Des.* **2020**, *20*, 4839–4844.
5. Stahly, G.P. Diversity in Single- and Multiple-Component Crystals. The Search for and Prevalence of Polymorphs and Cocrystals. *Cryst. Growth Des.* **2007**, *7*, 1007–1026.
6. Desiraju, G.R. Supramolecular Synthons in Crystal Engineering—A New Organic Synthesis. *Angew. Chem. Int. Ed.* **1995**, *34*, 2311–2327.
7. Wicker, J.G.P.; Crowley, L.M.; Robshaw, O.; Little, E.J.; Stokes, S.P.; Cooper, R.I.; Lawrence, S.E. Will they co-crystallize? *CrystEngComm* **2017**, *19*, 5336–5340.
8. Krishna, G.R.; Ukrainczyk, M.; Zeglinski, J.; Rasmuson, Å.C. Prediction of Solid State Properties of Cocrystals Using Artificial Neural Network Modeling. *Cryst. Growth Des.* **2018**, *18*, 133–144.
9. Devogelaer, J.J.; Meekes, H.; Tinnemans, P.; Vlieg, E.; Gelder, R. Co-crystal Prediction by Artificial Neural Networks. *Angew. Chem. Int. Ed.* **2020**, *59*, 21711–21718.
10. Zhang, S.-W.; Brunskill, A.P.J.; Schwartz, E.; Sun, S. Celecoxib–Nicotinamide Cocrystal Revisited: Can Entropy Control Cocrystal Formation? *Cryst. Growth Des.* **2017**, *17*, 2836–2843.
11. Perlovich, G.L. Formation Thermodynamics of Two-Component Molecular Crystals: Polymorphism, Stoichiometry, and Impact of Enantiomers. *Cryst. Growth Des.* **2020**, *20*, 5526–5537.
12. Musumeci, D.; Hunter, C.A.; Prohens, R.; Scuderi, S.; McCabe, J.F. Virtual cocrystal screening. *Chem. Sci.* **2011**, *2*, 883–890.
13. Báthori, N.B.; Lemmerer, A.; Venter, G.A.; Bourne, S.A.; Caira, M.R. Pharmaceutical Co-crystals with Isonicotinamide—Vitamin B3, Clofibric Acid, and Diclofenac—And Two Isonicotinamide Hydrates. *Cryst. Growth Des.* **2011**, *11*, 75–87.

14. Soares, F.L.F.; Carneiro, R.L. Green Synthesis of Ibuprofen–Nicotinamide Cocrystals and In-Line Evaluation by Raman Spectroscopy. *Cryst. Growth Des.* **2013**, *13*, 1510–1517.
15. Seaton, C.C.; Parkin, A.; Wilson, C.C.; Blagden, N. Controlling the Formation of Benzoic Acid: Isonicotinamide Molecular Complexes. *Cryst. Growth Des.* **2009**, *9*, 47–56.
16. Lemmerer, A.; Báthori, N.B.; Bourne, S.A. Chiral carboxylic acids and their effects on melting-point behaviour in co-crystals with isonicotinamide. *Acta Crystallogr. Sect. B Struct. Sci.* **2008**, *64*, 780–790.
17. Tothadi, S.; Desiraju, G.R. Unusual co-crystal of isonicotinamide: The structural landscape in crystal engineering. *Phil. Trans. R. Soc. A* **2012**, *370*, 2900–2915.
18. Seaton, C.C.; Parkin, A. Making Benzamide Cocrystals with Benzoic Acids: The Influence of Chemical Structure. *Cryst. Growth Des.* **2011**, *11*, 1502–1511.
19. Groom, C.R.; Bruno, I.J.; Lightfoot, M.P.; Ward, S.C. The Cambridge Structural Database. *Acta Crystallogr. Sect. B Struct. Sci.* **2016**, *72*, 171–179.
20. Bruno, I.J.; Cole, J.C.; Edgington, P.R.; Kessler, M.; Macrae, C.F.; McCabe, P.; Pearson, J.; Taylor, R. New software for searching the Cambridge Structural Database and visualizing crystal structures. *Acta Crystallogr. Sect. B Struct. Sci.* **2002**, *58*, 389–397.
21. Macrae, C.F.; Edgington, P.R.; McCabe, P.; Pidcock, E.; Shields, G.P.; Taylor, R.; Towler, M.; van de Streek, J. Mercury: Visualization and analysis of crystal structures. *J. Appl. Cryst.* **2006**, *39*, 453–457.
22. Macrae, C.F.; Bruno, I.J.; Chisholm, J.A.; Edgington, P.R.; McCabe, P.; Pidcock, E.; Rodriguez-Monge, L.; Taylor, R.; van de Streek, J.; Wood, P.A. Mercury CSD 2.0—New features for the visualization and investigation of crystal structures. *J. Appl. Cryst.* **2008**, *41*, 466–470.
23. Macrae, C.F.; Sovago, I.; Cottrell, S.J.; Galek, P.T.A.; McCabe, P.; Pidcock, E.; Platings, M.; Shields, G.P.; Stevens, J.S.; Towler, M.; et al. Mercury 4.0: From visualization to analysis, design and prediction. *J. Appl. Cryst.* **2020**, *53*, 226–235.
24. Weigend, F. Accurate Coulomb-fitting basis sets for H to Rn. *Phys. Chem. Chem. Phys.* **2006**, *8*, 1057–1059.
25. Weigend, F.; Ahlrichs, R. Balanced basis sets of split valence, triple zeta valence and quadruple zeta valence quality for H to Rn: Design and assessment of accuracy. *Phys. Chem. Chem. Phys.* **2005**, *7*, 3297.
26. Grimme, S.; Antony, J.; Ehrlich, S.; Krieg, H. A consistent and accurate ab initio parametrization of density functional dispersion correction (DFT-D) for the 94 elements H-Pu. *J. Chem. Phys.* **2010**, *132*, 154104.
27. Grimme, S.; Ehrlich, S.; Goerigk, L. Effect of the damping function in dispersion corrected density functional theory. *J. Comput. Chem.* **2011**, *32*, 1456–1465.
28. Neese, F. Software update: The ORCA program system, version 4.0. *WIREs Comput. Mol. Sci.* **2017**, *8*, e1327-6.
29. Zheng, J.; Xu, X.; Truhlar, D.G. Minimally augmented Karlsruhe basis sets. *Theor. Chem. Acc.* **2010**, *128*, 295–305.
30. Turner, M.J.; McKinnon, J.J.; Wolff, S.K.; Grimwood, D.J.; Spackman, P.R.; Jayatilaka, D.; Spackman, M.A. CrystalExplorer.
31. Price, K.V. Eliminating Drift Bias from the Differential Evolution Algorithm. In *Advances in Differential Evolution*; Springer: Berlin/Heidelberg, Germany, 2008; pp. 33–38.
32. Gavezzotti, A. Efficient computer modeling of organic materials. The atom–atom, Coulomb–London–Pauli (AA-CLP) model for intermolecular electrostatic-polarization, dispersion and repulsion energies. *New J. Chem.* **2011**, *35*, 1360–1368.
33. Svoboda, V.; MacFhionnghaile, P.; McGinty, J.; Connor, L.E.; Oswald, I.D.H.; Sefcik, J. Continuous Cocrystallization of Benzoic Acid and Isonicotinamide by Mixing-Induced Supersaturation: Exploring Opportunities between Reactive and Antisolvent Crystallization Concepts. *Cryst. Growth Des.* **2017**, *17*, 1902–1909.
34. Aakeröy, C.B.; Beatty, A.M.; Helfrich, B.A. A High-Yielding Supramolecular Reaction. *J. Am. Chem. Soc.* **2002**, *124*, 14425–14432.
35. Vishweshwar, P.; Nangia, A.; Lynch, V.M. Molecular Complexes of Homologous Alkanedicarboxylic Acids with Isonicotinamide: X-ray Crystal Structures, Hydrogen Bond Synthons, and Melting Point Alternation. *Cryst. Growth Des.* **2003**, *3*, 783–790.